Supplementary Information

Sorting sub-150-nm liposomes of distinct sizes by DNA-brick assisted centrifugation

Yang Yang, Zhenyong Wu, Laurie Wang, Kaifeng Zhou, Kai Xia, Qiancheng Xiong, Longfei Liu, Zhao Zhang, Edwin R Chapman, Yong Xiong, Thomas J Melia, Erdem Karatekin, Hongzhou Gu and Chenxiang Lin

Contents

Supplementary Tables

Supplementary Table 1. DNA strand sequences

3 Point Star Brick (3PS bricks)	
Name	Sequence
C	AGGCATATTGAATCGTTTACAGGATTAGTAATTAACAGCTTTAATATCATCGCCCATCGTAGGTTTCTTGCC
C-Cy5	/5Cy5/AGGCATATTGAATCGTTTACAGGATTAGTAATTAACAGCTTTAATATCATCGCCCATCGTAGGTTTCTTGCC
S-a	GACGACAGAGGTTGCTAGGCG
S-b	TTACCGTGTGTGTTAAGGTGG
S-c	ACCGAGCCTCCGTCAACATCG
E-a	CCACCTTAACACGCGATGATATTGCTGTTAATTAGGCTCGGT
E-b	CGATGTTGACGGACTAATCCTGTCGATTCAATATCTGTCGTC
E-0	CGCCTAGCAACCTGCCTGGCAAGCCTACGATGGACACGGTAA
E-Chol	CGCCTAGCAACCTGCCTGGCAAGCCTACGATGGACACGGTAA/3CholTEG/
6 Helix Bundle Brick (6HB bricks)	
6hb-M0	TTTAGTGCTACACTGTGCGTATGCGAAAACTTGCGATATGCTCCATTT
6hb-M1	TTTAGTCGAGTGAACTGTAACGTACAGGTAGATAGACTCTGTATCTTT
6hb-M2	AAATTATCTACCACAACTCACCGCCTAGCAACCTGCCTGGCAAGCCTACGATGGACACGGTAA
6hb-M3	TTTATTCGAGCATGTCAGTGGATCAATCGTGTTAGACATGACGTATTT
6hb-M4	TTTGTGGACTATATATACGTGGAACCATGAATTGGCTGAGTTTGGTTT
6hb-M5	TTTTGGTTTACTCACTATTGTCACCTTATACCACAATCAGATCCGTTT
6hb-S0	CACAGTGGATTGTGTATATATAGTCCACTACGTCACTAGGCG
6hb-S1	CAGTTCAGTCCATCTGACATGCTCGAATCCAAACTTAAACCA
6hb-S2	TTACCGTCTCGACTTGGAGCATATCGCATAGTGAGCAGCCAA
6hb-S3	CACGATTTTCCACGGTATAAGGTGACAAAGTTTTCTACGTTA
6hb-S3-Cy5	/5Cy5/CACGATTTTCCACGGTATAAGGTGACAAAGTTTTCTACGTTA
6hb-S4	TTCATGGGATCCACGTAGGCTTGCCAGGCTACCTGGCATACG
6hb-S5	CGGATCTTAGCACTGATACAGAGTCTATCAGGTTGTGTCTAA
M2'-Chol	GTGAGTTGTGGTAGATAATTT/3CholTEG/
Deoxyribozyme	
I-R1a-FAM	/56FAM/CATGTACAGCCATAGTTGAGCATTAAGTTGAAGTGGCTGTACATG

Supplementary Table 2. Lipid compositions and buffer ingredients. Numeric values refer to molar percentages and ratios. Composition B is used in this work unless noted otherwise.

Abbreviation	Full name of lipids
DOPC	1,2-dioleoyl-sn-glycero-3-phosphocholine
DOPE	1,2-dioleoyl-sn-glycero-3-phosphoethanolamine
DOPS	1,2-dioleoyl-sn-glycero-3-phospho-L-serine
DOTAP	1,2-dioleoyl-3-trimethylammonium-propane
PEG-2k-DOPE	1,2-dioleoyl-sn-glycero-3-phosphoethanolamine-N-[methoxy(polyethylene glycol)-2000]
rhodamine-DOPE	1,2-dioleoyl-sn-glycero-3-phosphoethanolamine-N-(lissamine rhodamine B sulfonyl)
POPC	1-palmitoyl-2-oleoyl-glycero-3-phosphocholine
NBD-DOPE	1,2-dioleoyl-sn-glycero-3-phosphoethanolamine-N-(7-nitro-2-1,3-benzoxadiazol-4-yl)
POPE	1-palmitoyl-2-oleoyl-sn-glycero-3-phosphoethanolamine
PIP2	phosphatidylinositol 4,5-bisphosphate

	DOPC	DOPE	DOPS	DOTAP	PEG-2k-DOPE	rhodamine-DOPE
Composition A	99.2%	0%	0%	0%	0%	0.8%
Composition B	59.2%	30%	10%	0%	0%	0.8%
Composition C	59.2%	30%	0%	10%	0%	0.8%
Composition D	94.2%	0%	0%	0%	5%	0.8%

	POPC	DOPS	rhodamine-DOPE	NBD-DOPE	v-SNARE:lipid
v-SNARE liposome	82%	15%	1.5%	1.5%	1:200, 1:300 or 1:400
	POPC	DOPS	POPE	PIP2	t-SNARE:lipid
t-SNARE liposome	58%	25%	15%	2%	1:400

	HEPES	KCl	$MgCl_2$	pH
Buffer X	25 mM	400 mM	10 mM	7.0
Buffer Y	25 mM	140 mM	0 mM	7.0

Supplementary Table 3.
The amount of reagents used for different scale of sorting experiments.

Scale	Brick amount	Lipid amount	Total volume	Volume loaded to iodixanol gradient
1×	40 pmol	15 nmol	45 μL	45 μL + 45 μL 45% iodixanol
10×	400 pmol	150 nmol	350 μL	350 μL + 350 μL 45% iodixanol
20×	800 pmol	300 nmol	350 μL	350 μL + 350 μL 45% iodixanol

Supplementary Table 4.
Size ranges of the sorted liposome and their expected locations after fractionation.

3PS-brick assisted sorting (1:1 mixture of extruded & sonicated liposomes, composition B)

Mean liposome diameter (nm)	>120	80–120	60–80	40–60	30–40	<30
Expected fractions	F4–8	F9–10	F11–13	F14–15	F16–17	F18-20

3PS-brick assisted sorting (reconstituted proteoliposomes, v-SNARE:lipid = 1:200)

Mean liposome diameter (nm)	>100	80–100	70–80	60–70	50–60	40–50	<40
Expected fractions	F3–4	F5–6	F7–8	F9–10	F11–12	F13–14	F15–18

Supplementary Table 5.
NBD fluorescence (mean and SD) measured at different lipid dilution factors.

Colored: clear lipid stock ratio	1:0	1: 0.5	1: 1	1:2	1:4	1:8
Dilution factor (folds)	1	1.5	2	3	5	9
Normalized NBD fluorescence (%), N=3	0	9.993	19.264	39.835	58.789	80.76
SD (%), N=3	0	0.53	0.58	0.48	1.05	1.74

Supplementary Figures

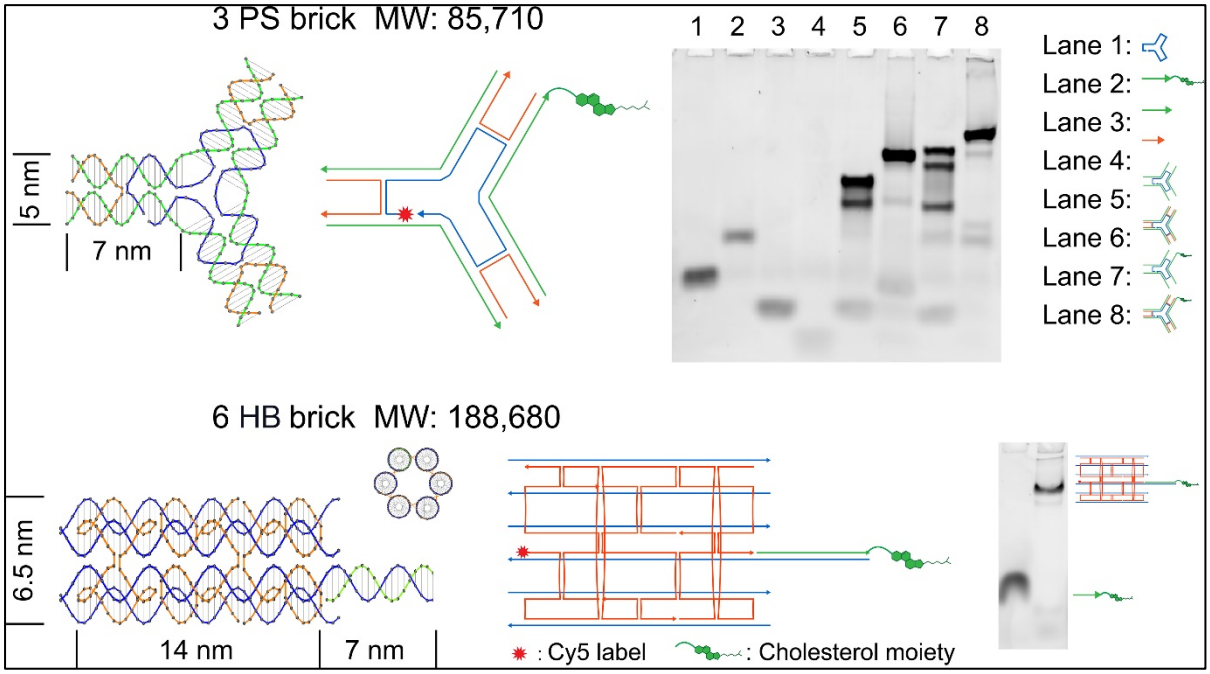

Supplementary Figure 1. (a) 3 Point Star (3PS) and (b) 6 Helix Bundle (6HB) DNA bricks. Design diagrams are shown to the left of native PAGE results (6% gel run at 15 V/cm for 70 min). The experiment was repeated 3 times with similar results.

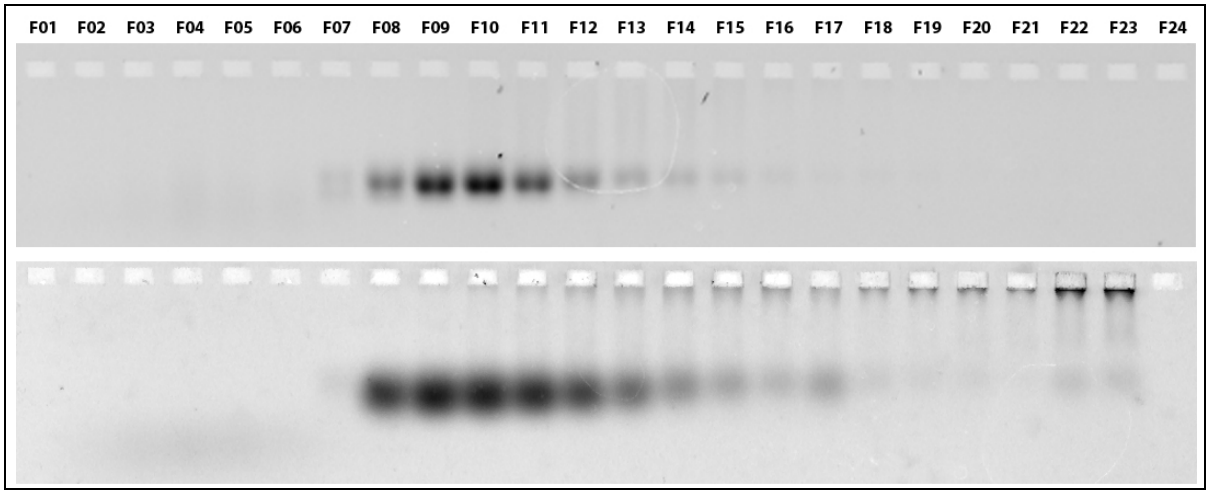

Supplementary Figure 2. Representative images of agarose gels showing DNA bricks (top: 3PS; bottom: 6HB) after rate-zonal centrifugation. Fractions 1–24 (F01, F02 … F24) were collected from the top to the bottom of the glycerol gradient. The experiment was repeated more than 20 times for both brick types with satisfactory separation each time.

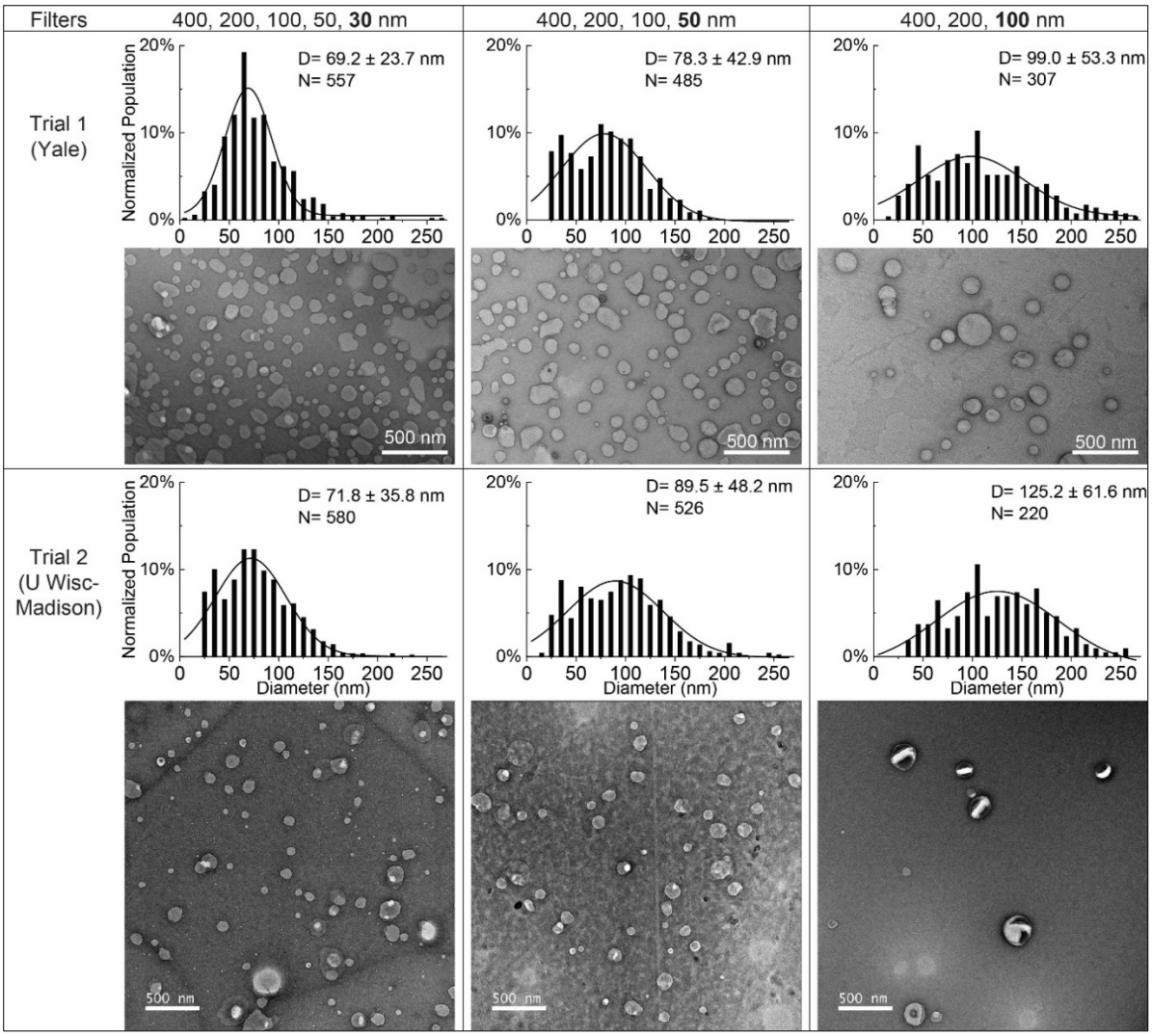

Supplementary Figure 3. Size distributions and representative negative-stain transmission electron microscopy (TEM) images of sequentially extruded liposomes (Composition B in Buffer Y, **Supplementary Table 2**). Extrusion filter pore sizes are noted on top of each column with the final-pass filter size shown in bold letters. Two trials following the same protocol were performed at two labs (at Yale and Wisconsin-Madison) using lipids and filters purchased from the same source. TEM grids were prepared (Method *4b*) immediately following liposome extrusion.

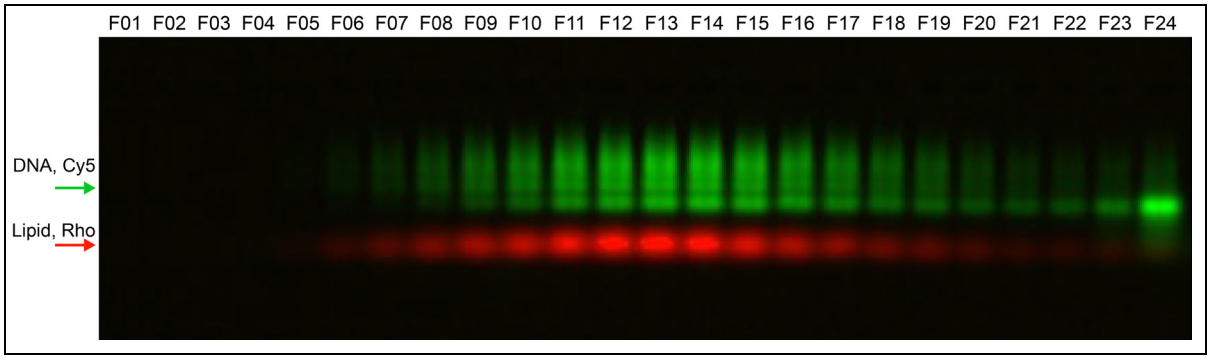

Supplementary Figure 4. A typical SDS-agarose gel analysis showing the distribution of DNA-coated liposomes in the iodixanol gradient after isopycnic centrifugation. F01–F24 denotes the fractions collected from top to the bottom of the gradient. Pseudo-color green: Cy5-labeled DNA bricks, red: rhodamine-labeled lipids. Before running in this gel, a pool of extruded liposomes (300 pmol of total lipid, 50-nm pore size) were sorted with the help of 3PS bricks as described above. Notice that the heaviest fraction (F24) contains a large amount of DNA bricks with a negligible amount of lipids, suggesting surface saturation on most liposomes. The liposomes were lysed by SDS in the gel and running buffer, causing the lipid bands to migrate faster than the DNA-brick bands. The experiment was repeated more than 10 times with similar results.

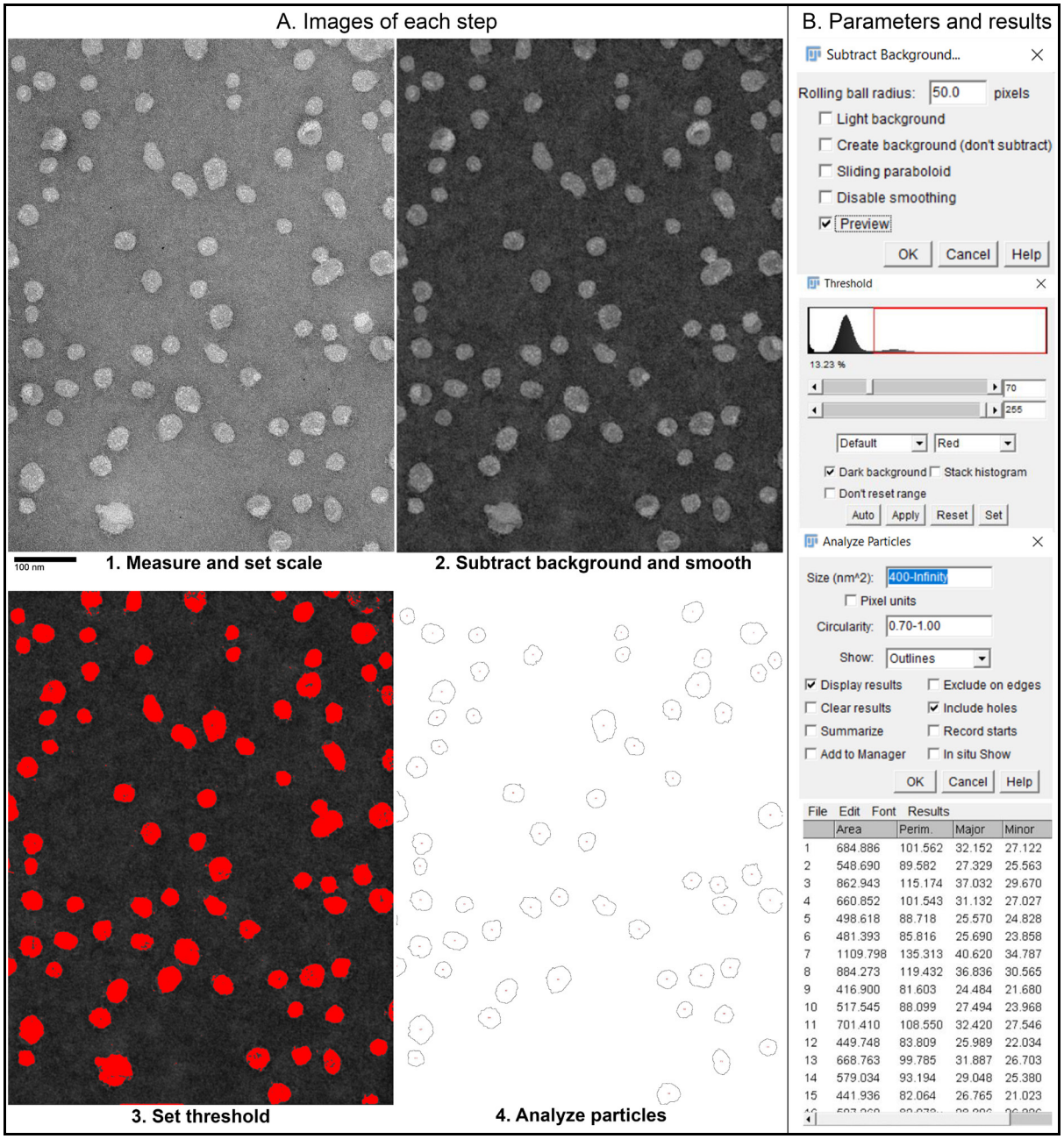

Supplementary Figure 5. TEM image analysis pipeline to determine the diameters of sorted liposomes using the built-in functions of ImageJ. The steps are: 1. Set scale by measuring the length of the scale bar; 2. Subtract background (Rolling ball radius was set in the range of 50–150 depending on the original contrast) and smooth image (10×) for contrast enhancement and noise reduction; 3. set threshold at an appropriate value to highlight all the liposomes (holes inside are acceptable); 4. run particle analysis (circularity higher than 0.7, show outlines, include holes and display results as listed). Finally, the diameter of each liposome is calculated based on the measured area (*A*) following the equation: $\mathrm{D} = 2 \times \sqrt{\mathrm{A}/\pi}$. Parameter setups are illustrated in panel B on the right. This method was used to measure virtually all liposome samples imaged by TEM (i.e. repeated more than 150 times) whenever the sample has sufficient contrast and concentration.

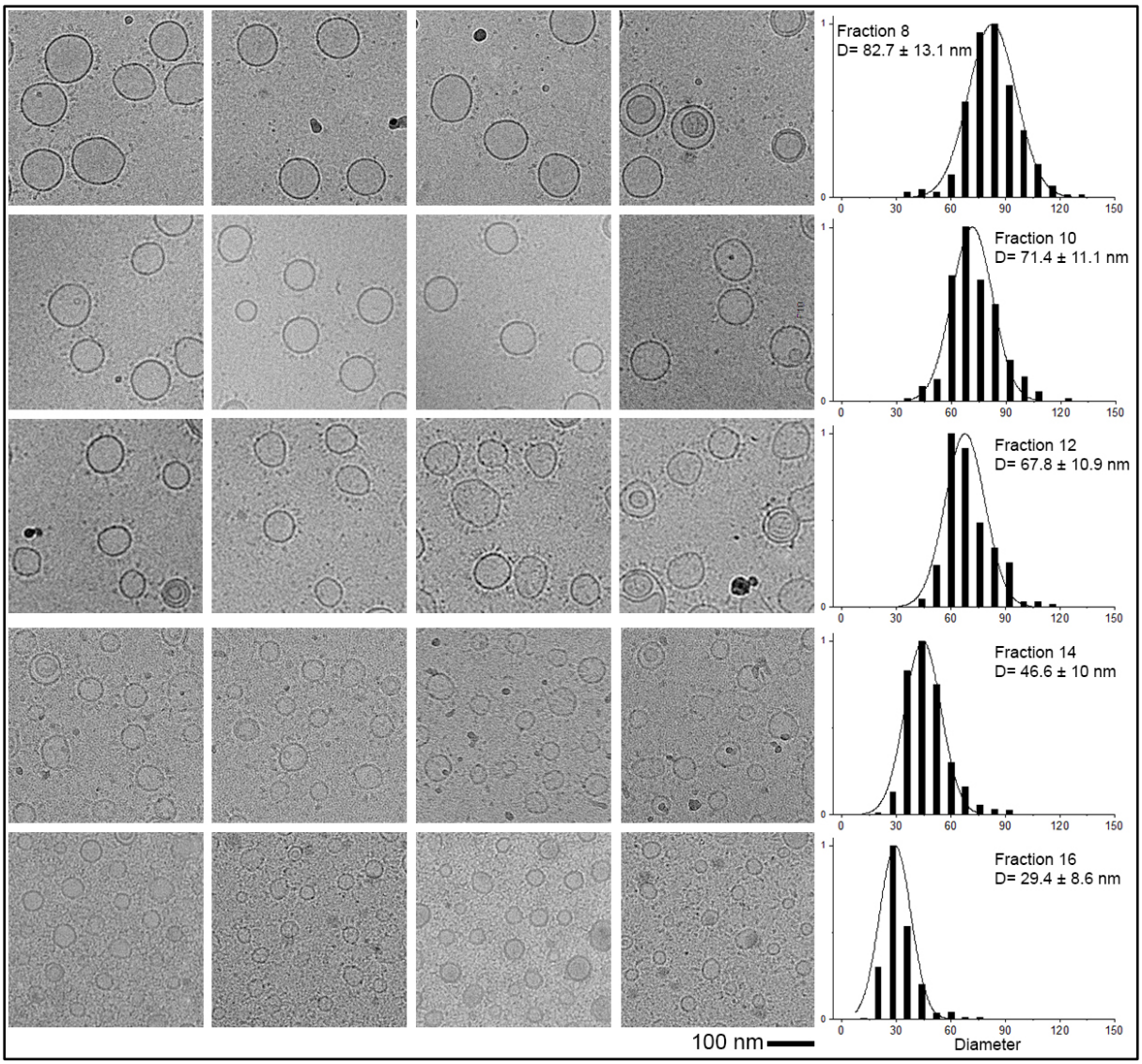

Supplementary Figure 6. Cryo-EM images of liposomes after sorting. Representative micrographs of fractions 8, 10, 12, 14 and 16 are shown from top to bottom, together with the corresponding histograms showing the liposome size distributions (liposome diameter D=mean±SD, n=252, 328, 235, 408, 474 from top to bottom). The six-helix bundle bricks are visible on the exterior surface of the liposomes. Scale bar: 100 nm.

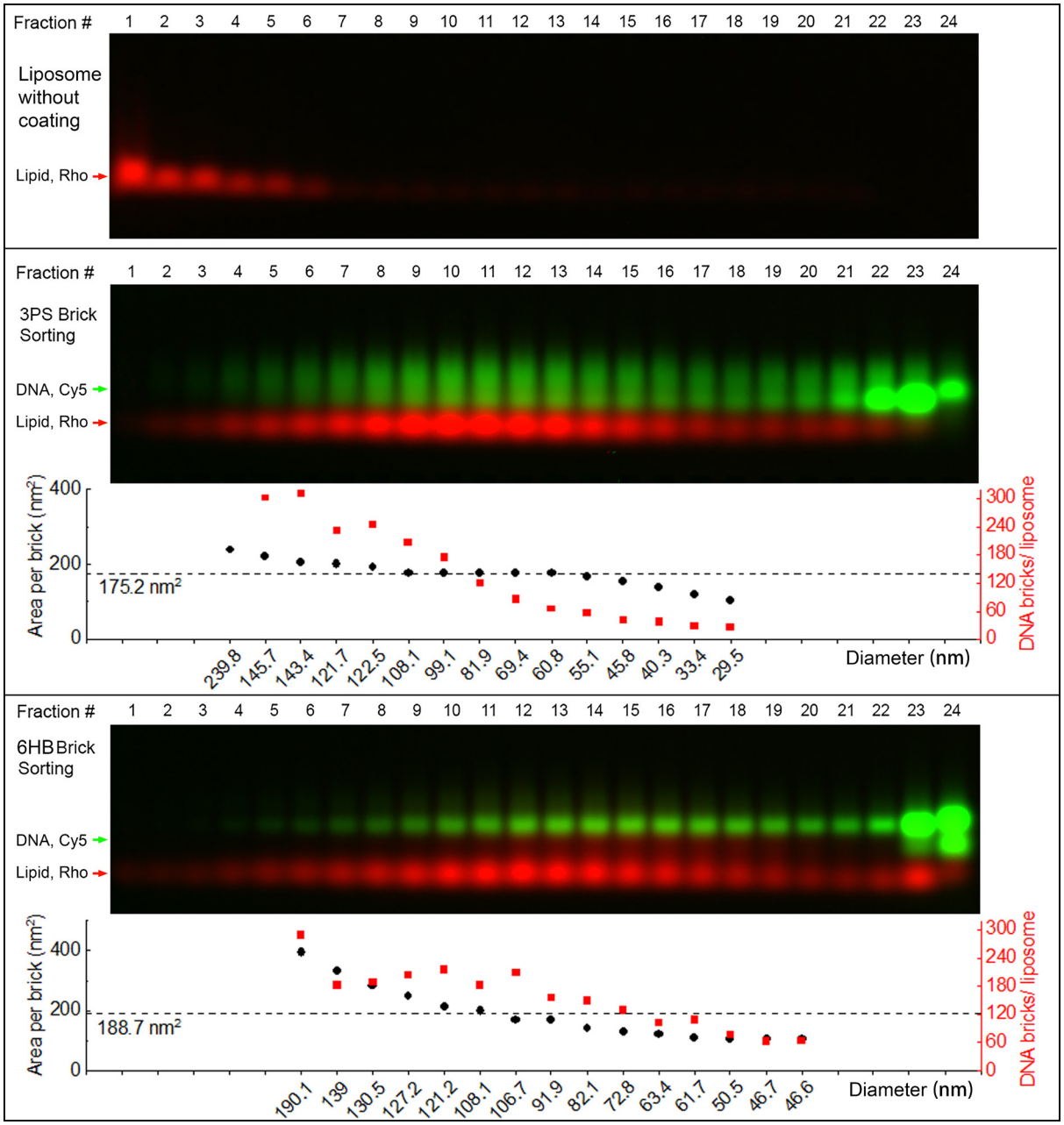

Supplementary Figure 7. Uncoated (top) and 3PS-(middle)/6HB-(bottom) brick coated liposomes after ultracentrifugation in iodixanol density gradients (Method **3**). Fractions are electrophoresed in the same SDS-agarose gel (Method *4a*). Liposomes to be sorted consist of a 1:1 (molar ratio of total lipid) mixture of extruded (through 50-nm pores) and sonicated liposomes. The average surface area occupied by each brick is calculated based on lipid:DNA ratio estimated from the band intensities. On average, each brick occupied ~200 nm^2 of membrane surface. Bricks bound stronger to smaller liposomes, presumably because of more lipid packing defects in the highly curved membranes. These experiments were repeated more than 10 times with similar results, however only the bottom two gels shown here were quantitatively analyzed.

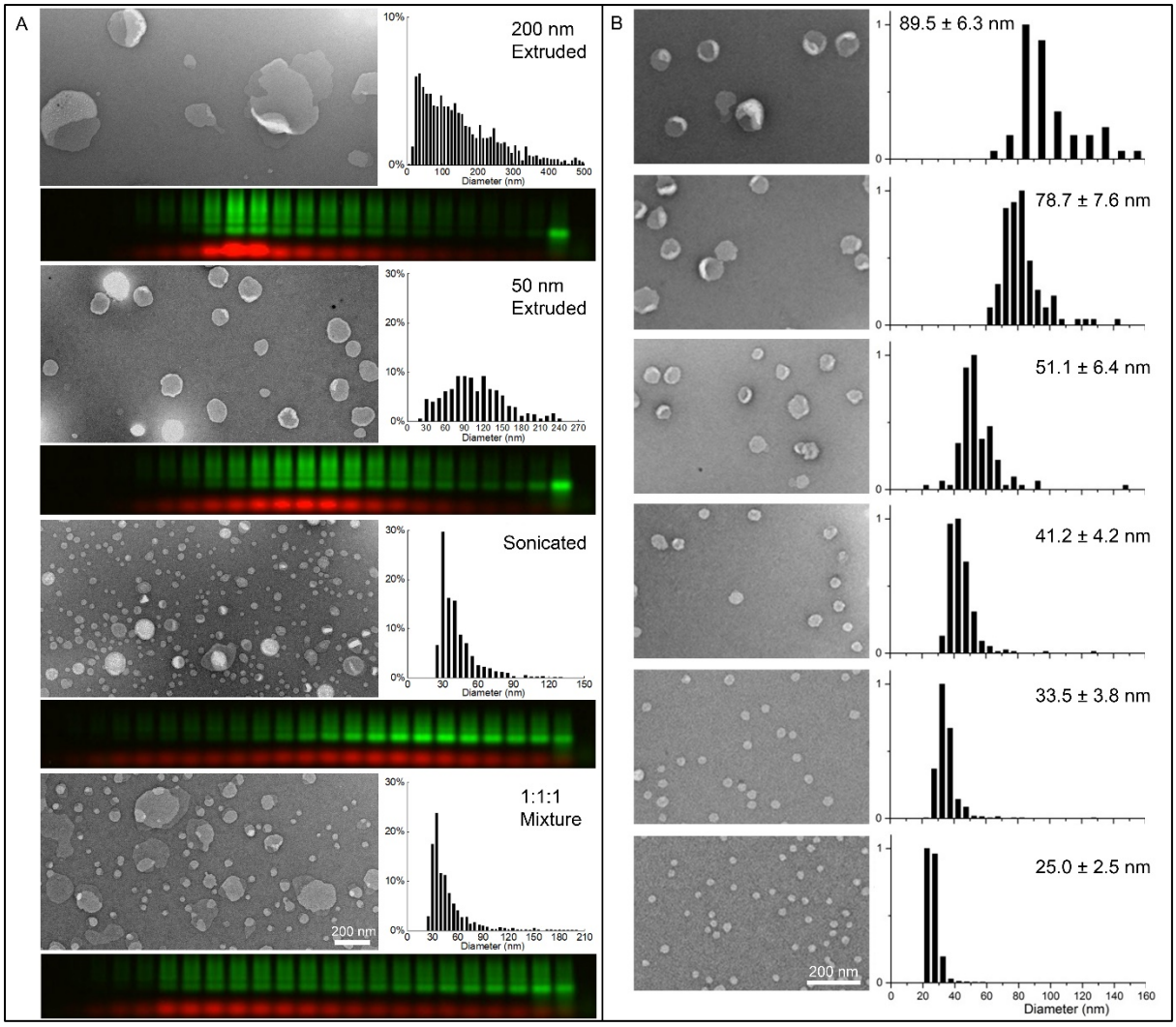

Supplementary Figure 8. DNA-brick assisted sorting of liposomes of different origins and size distributions. (A) Various heterogeneous liposomes (extruded liposomes, sonicated liposomes, and their mixture) and the sorting results (analyzed by SDS-agarose gel electrophoresis). For each sample, a representative TEM image, a histogram of liposome diameters (mean±SD, n=637, 251, 1349, 1926 from top to bottom), and a pseudo-colored agarose gel (red: rhodamine-labeled lipid, green: Cy5-labeled DNA) containing 3PS-brick assisted sorting products are shown. The distributions of rhodamine fluorescence within the gradients reflect the spectra of liposome size before sorting. The diameter histogram of the 1:1:1 (molar ratio of total lipid) liposome mixture is similar to that of the sonicated liposomes because of a dominant population of <40-nm liposomes in the 1:1:1 mixture. (B) Representative TEM images and diameter histograms (mean±SD, n=54, 104, 118, 257, 525, 1004 from top to bottom) of liposomes sorted from the 1:1:1 mixture with the help of 3PS bricks. Scale bar: 200 nm.

Note: Reconstituted liposomes can be sorted successfully as well (**Supplementary Figure 21**).

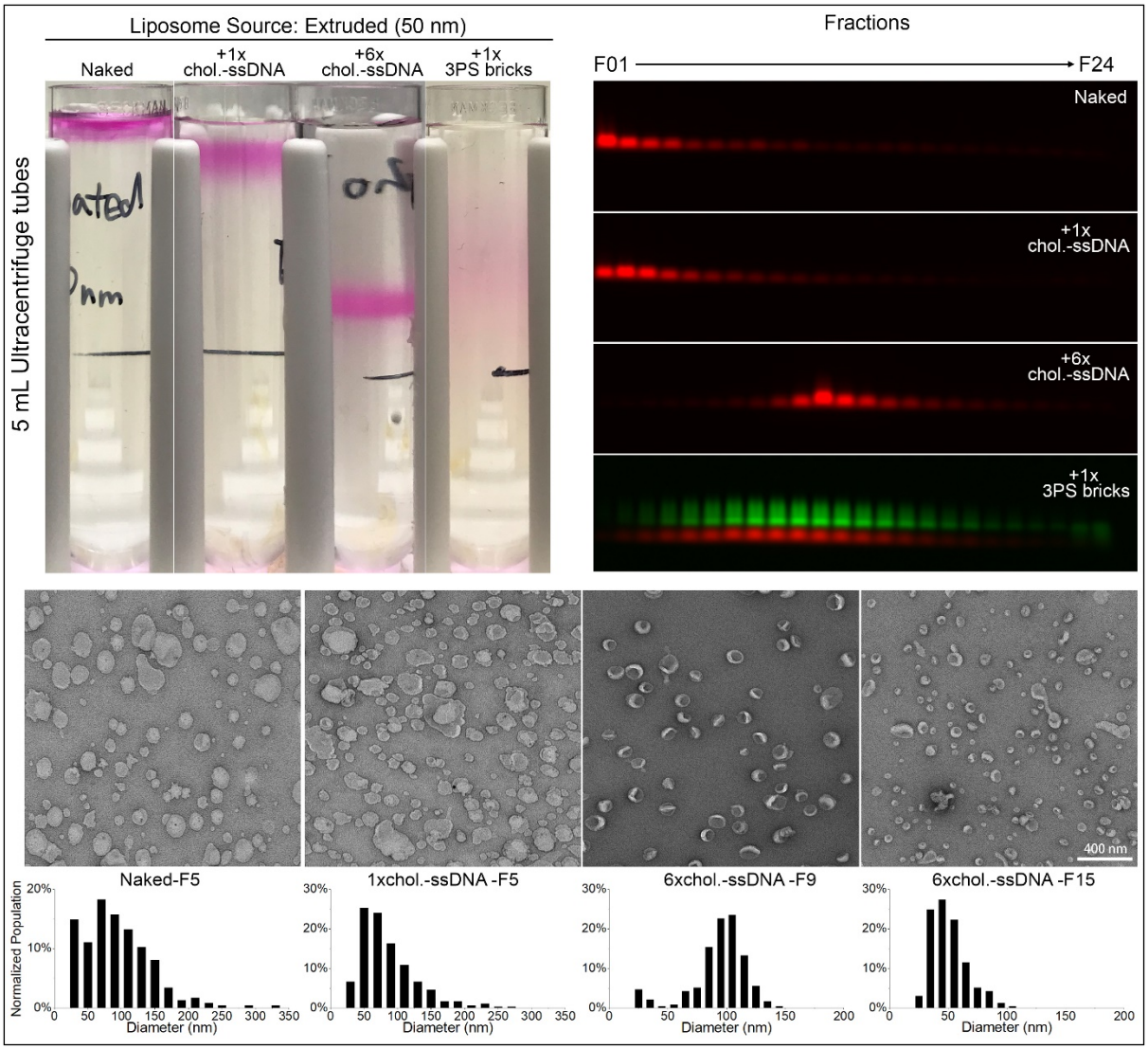

Supplementary Figure 9. Control experiments that attempt to sort extruded liposomes (50-nm pore size) by the same gradient-centrifugation method (Method *3b*) but with only cholesterol-labeled ssDNA (chol-ssNDA) coating instead of DNA brick coating (repeated 3 times with similar results). Pictures of the gradient (top left, rhodamine-labeled liposomes appear pink), as well as electrophoresis (top right, red: rhodamine-labeled lipid, green: Cy5-labeled DNA) and TEM (bottom) analyses indicate ineffective liposome separation in the gradient and co-migration of hetero-sized liposomes. In liposome diameter histograms, n=235, 349, 234, 234 from left to right. Scale bar: 400 nm.

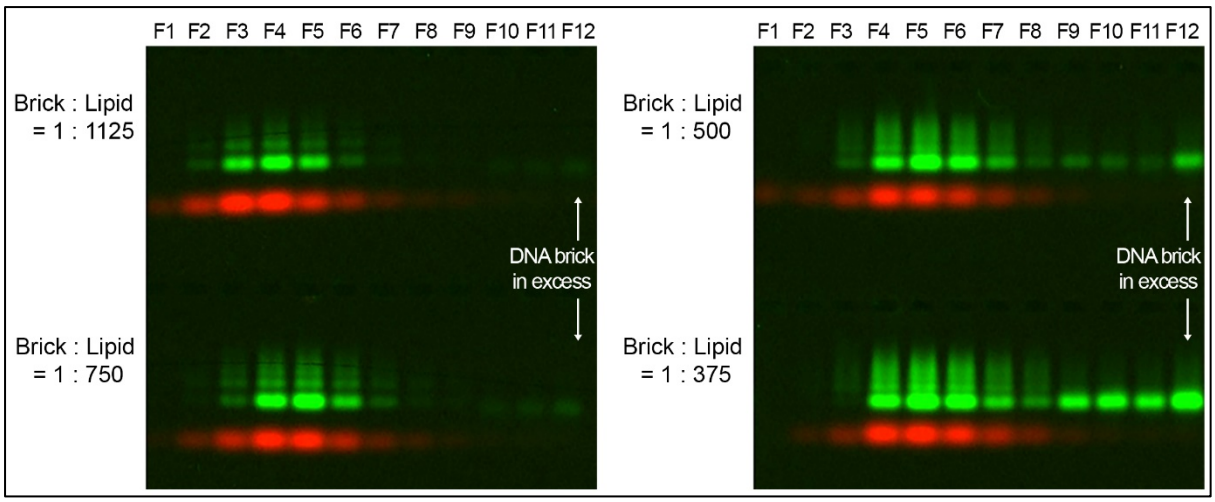

Supplementary Figure 10. Liposome sorting with various DNA brick to lipid ratios. Sorting was performed at 1× scale (see **Supplementary Table 3**) with the same total lipid amount (15 nmol) and various amount of 3PS DNA brick (at 13.3, 20, 30, 40 pmol). The sorting results (analyzed by SDS-agarose gel electrophoresis) show a wider spread of liposomes (pseudo-color red) in the gradient and more free DNA bricks (pseudo-color green) in the heaviest fraction (F12) with increasing amount of DNA bricks. A brick:lipid molar ratio of 1:375 was chosen for the rest of sorting experiments to ensure the saturation of membranes without wasting too much material. Subsequent sorting experiments (>10 trials) were performed using a 1:375 brick:lipid ratio with similar results. The other brick:lipid ratios were deemed suboptimal and thus not repeated.

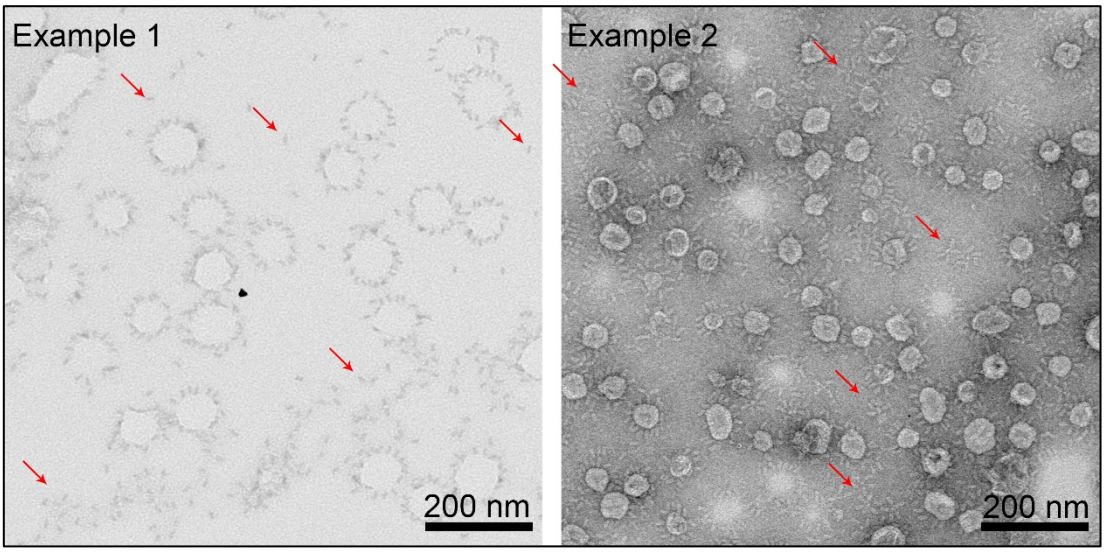

Supplementary Figure 11. Detached 6HB DNA bricks (marked by red arrows) from sorted liposome. Free 6HB bricks are visible in electron micrographs under both positive-stain (example 1) and negative-stain (example 2) conditions. This phenomenon was observed in >20% negative-stained areas and >90% of positive-stained areas of the ~100 TEM grids imaged.

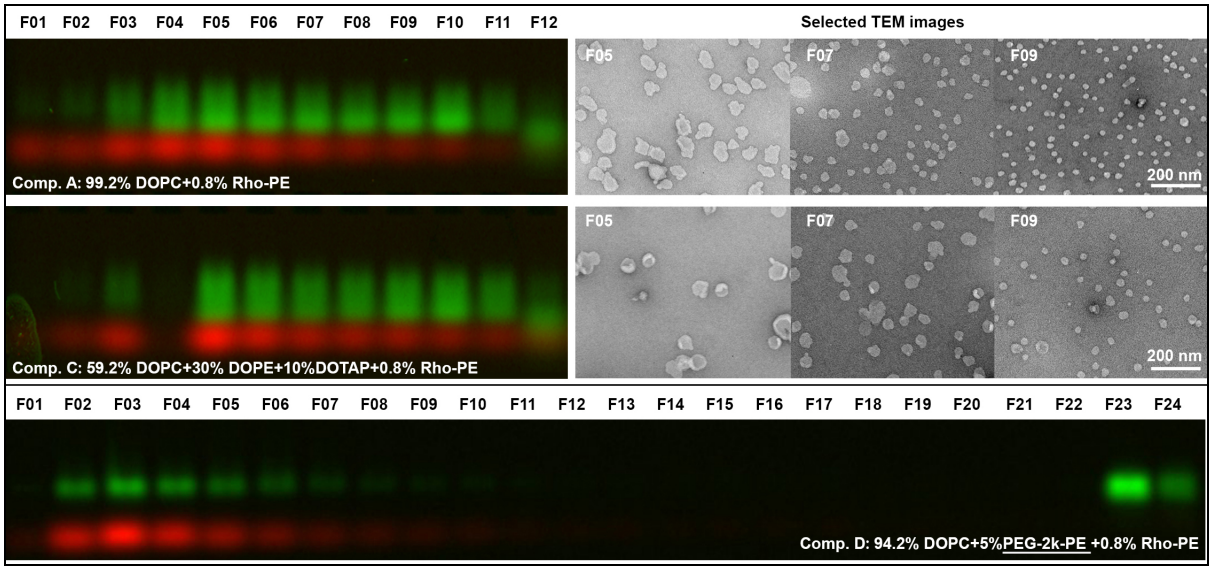

Supplementary Figure 12. DNA-brick (3PS) assisted sorting of liposome of different lipid compositions. Top row: small scale (1×, **Supplementary Table 3**) sorting of liposomes of Composition A (**Supplementary Table 2**). A pseudo-colored SDS-agarose gel (red: rhodamine-labeled lipid, green: Cy5-labeled DNA) containing density-gradient fractions is shown to the left of the representative TEM images (scale bar: 200 nm). Middle row: same as top row, but with Composition C. The changes in lipid charge do not have a major impact on sorting results. Bottom row: Attempted large scale (10×, **Supplementary Table 3**) sorting of liposomes with Composition D. The PEGylated lipids (PEG-2k-DOPE, **Supplementary Table 2**) hamper DNA-brick coating and thus negatively impact sorting. Liposomes sorting for lipid compositions A and C was repeated twice with similar results (see **Supplementary Figure 13**). Sorting was deemed ineffective and thus not attempted again for liposomes with lipid composition D.

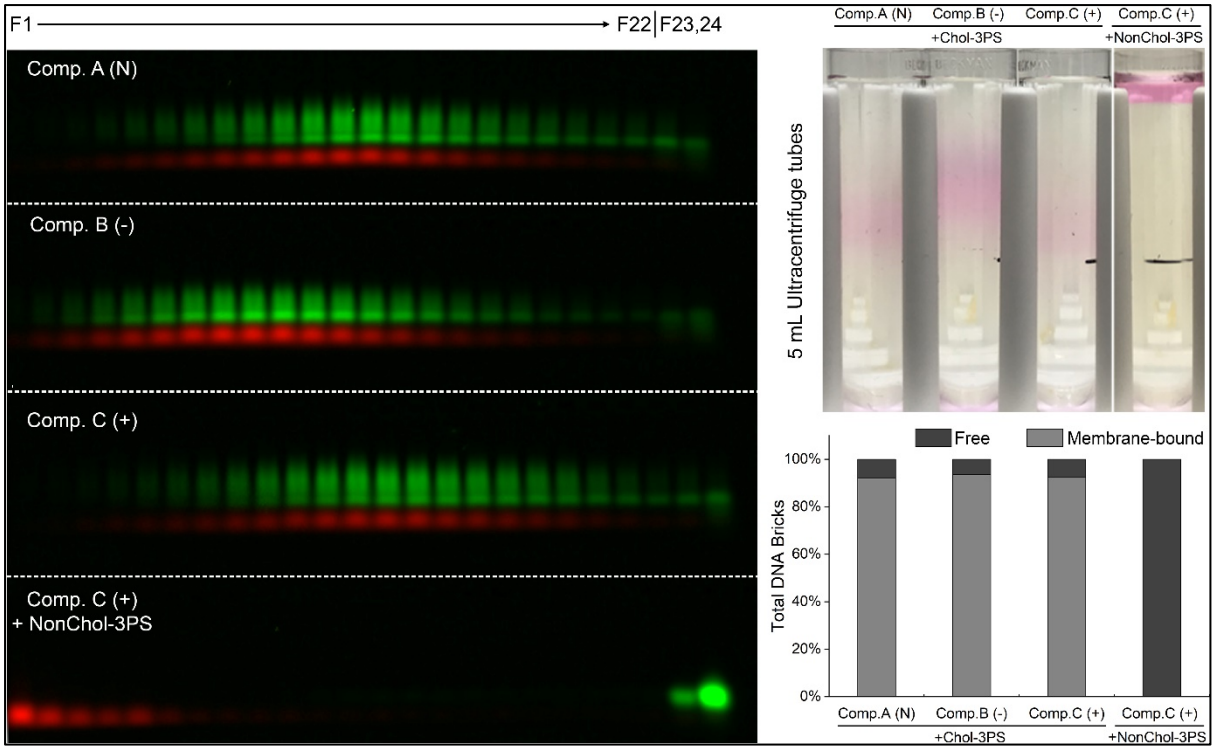

Supplementary Figure 13. Large scale (20×, **Supplementary Table 3**) sorting of liposomes of different lipid compositions with the help of 3PS bricks. Left: Pseudo-colored SDS agarose gel images (red: rhodamine-labeled lipid, green: Cy5-labeled DNA) containing post-centrifugation density-gradient fractions. Top right: pictures of the density gradients from which the electrophoresed fractions are recovered. Rhodamine-labeled liposomes appear pink. Bottom right: quantification of membrane-bound (in F1-F22) and membrane-free (F23-F24) bricks in each post-centrifugation gradient. Note that in the gradient where cholesterol-free DNA bricks were incubated with positively charged liposomes (Comp. C, +NonChol-3PS), there is no detectable membrane-bound brick and very little separation of liposomes. Liposome sorting for lipid compositions A and C was repeated twice with similar results (see **Supplementary Figure 12**). Sorting with cholesterol-free DNA bricks was deemed ineffective and thus not attempted again.

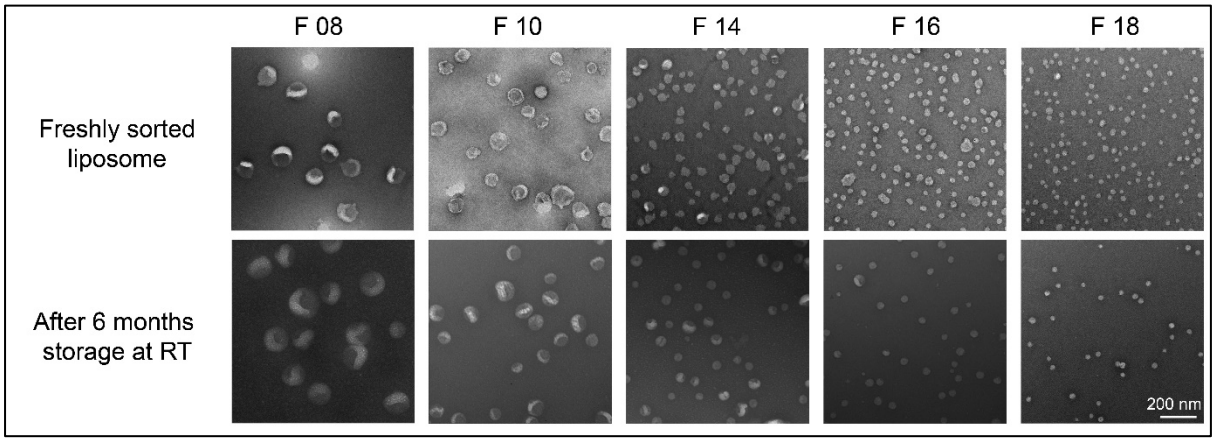

Supplementary Figure 14. Stability of the sorted liposomes. TEM images of freshly sorted liposomes with 3PS-brick coating (top) and those after 6-month storage at room temperature (bottom) show comparable size homogeneity. Notice that the liposomes in F14, F16 and F18 have considerably smaller concentration after long-term storage. This experiment was not repeated because of the time-consuming sample preparation.

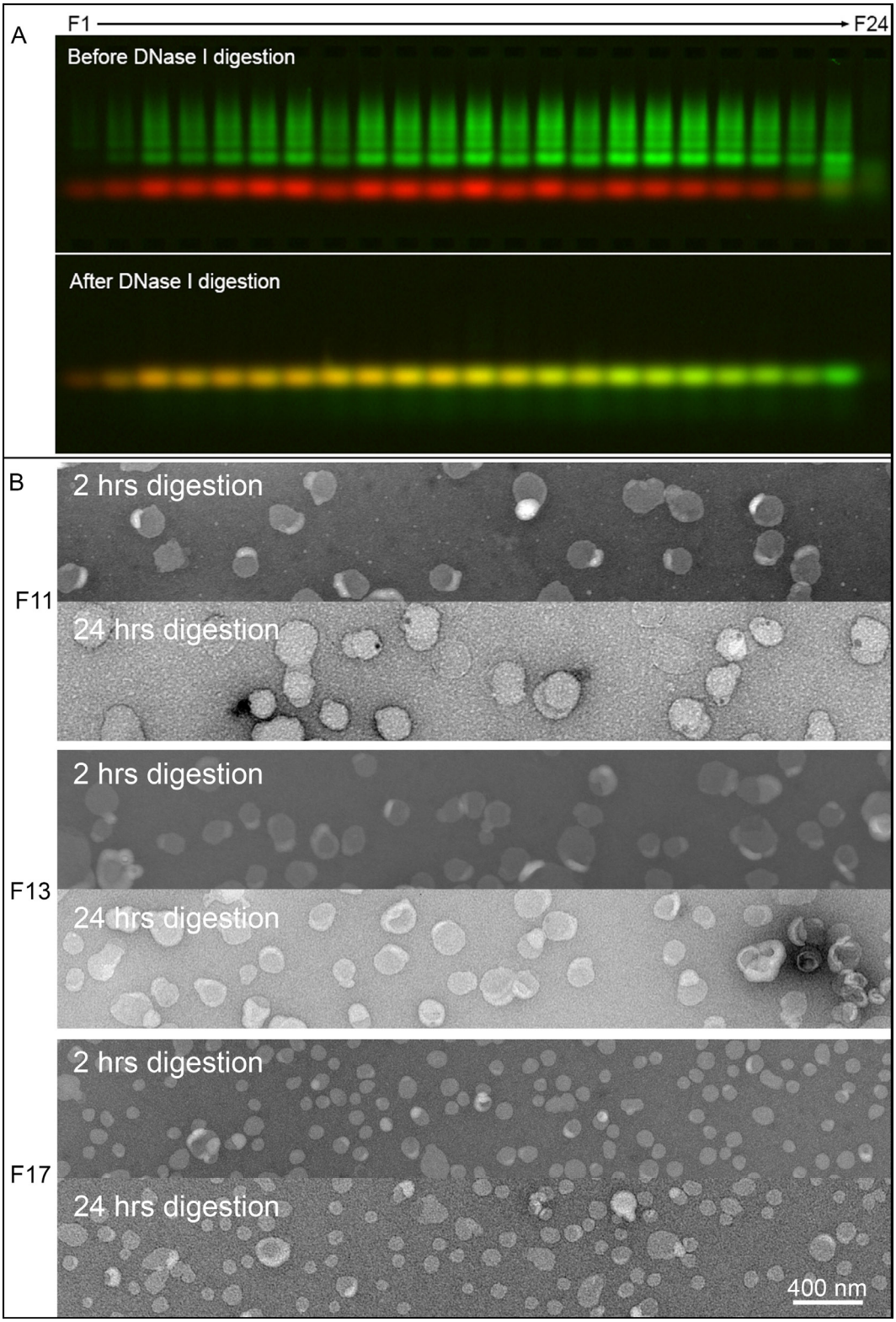

Supplementary Figure 15. Enzymatic removal of DNA bricks from sorted liposomes. (A) SDS-agarose gel analyses of sorted liposomes before (top) and after (bottom) nuclease treatment. One unit of DNase I is added to 100 μL of fractionated liposomes (coated by 3PS brick) and incubated at 37°C for 24 hours. Pseudo-color green: Cy5-labeled DNA, red: rhodamine-labeled lipid. (B) TEM images of selected fractions (F11, F13 and F17) showing liposomes treated by DNase I for 2 or 24 hours. This experiment was repeated 3 times with similar results.

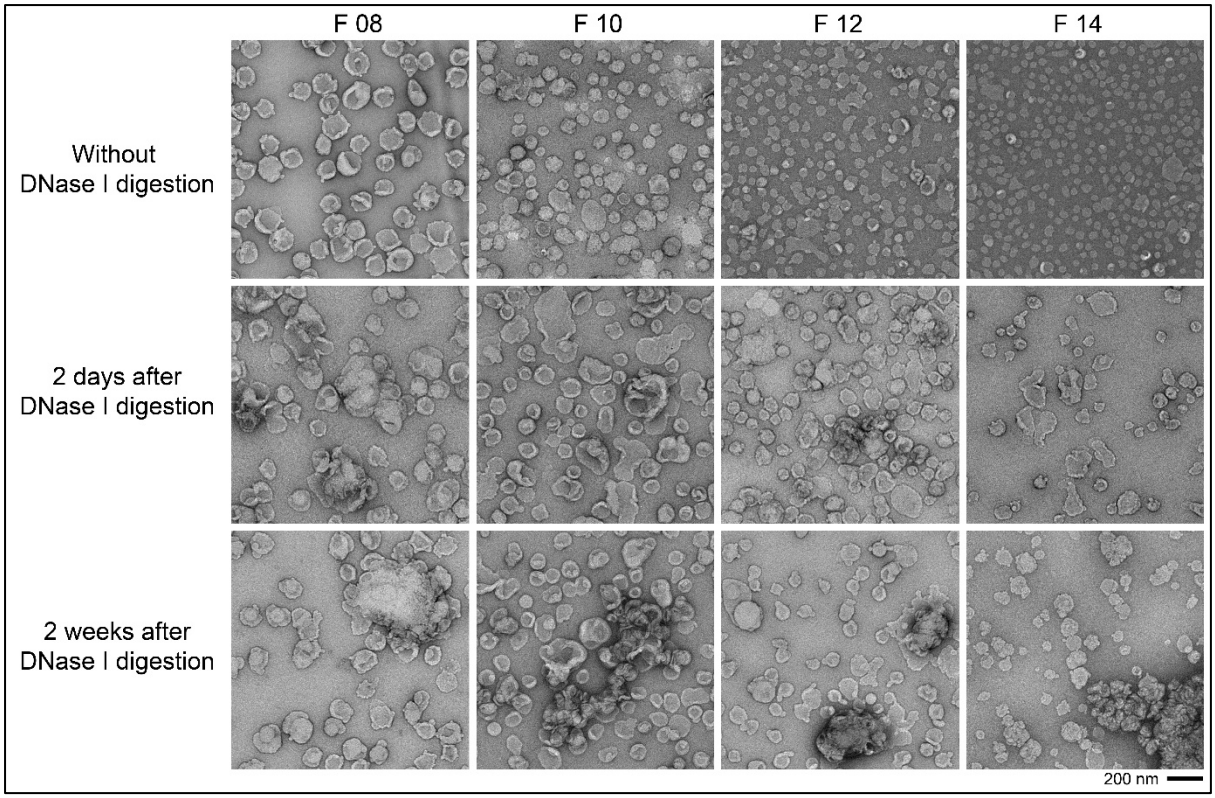

Supplementary Figure 16. TEM images of sorted liposomes (coated by 3PS brick) before and after DNase I digestion. Notice the aggregated and fused liposomes as soon as 2 days after the removal of DNA coats. This experiment was repeated twice with similar results.

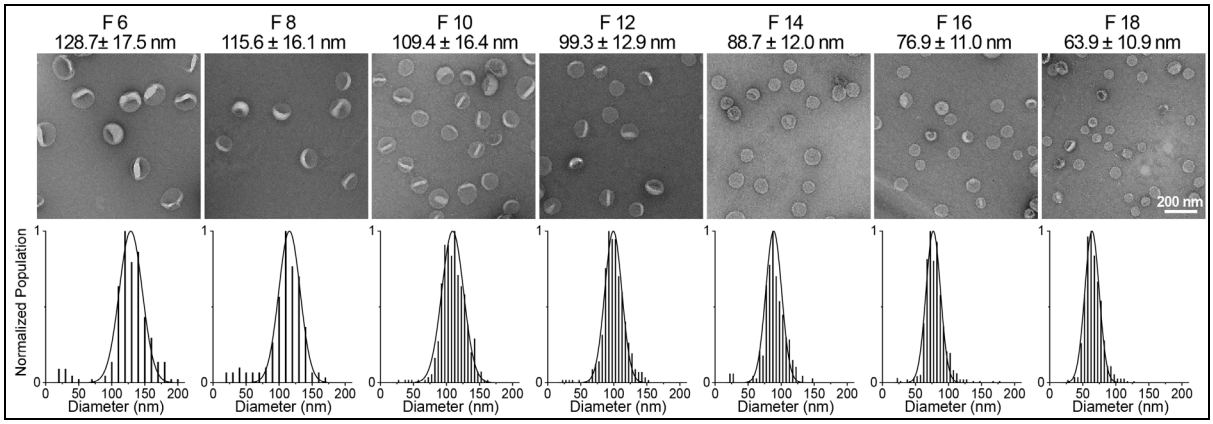

Supplementary Figure 17. 6HB-brick assisted sorting of deoxyribozyme encapsulating liposomes. For sorted liposomes in each fraction, a representative TEM image is shown on top of the corresponding histogram of diameters. Liposomes contain deoxyribozyme I-R1a and are sorted with the help of 6HB bricks. Scale bar: 200 nm.

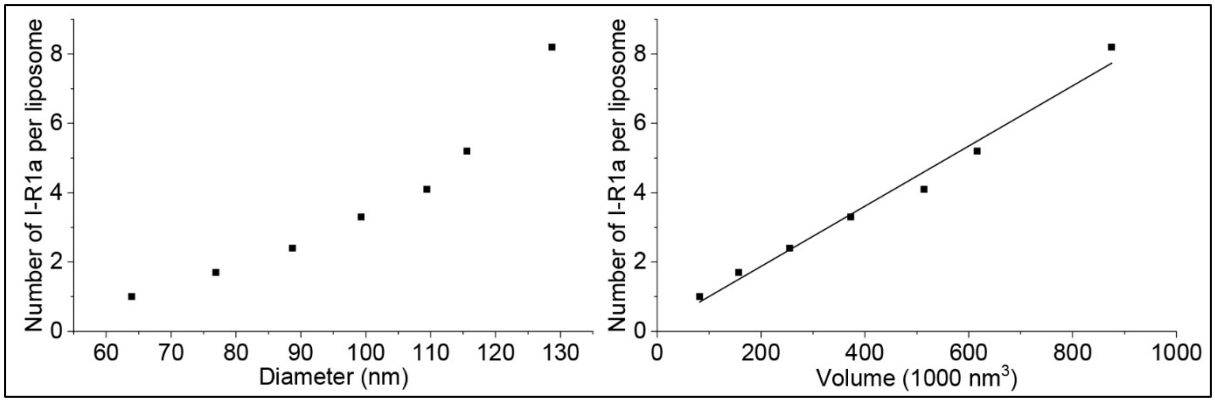

Supplementary Figure 18. Average number of deoxyribozymes (I-R1a) per liposome plotted as a function of liposome diameter (left) and volume (right). Overall, only ~1% of the total I-R1a were packaged into liposomes (3 mM lipid) and recovered after sorting. This is expected, because the encapsulation here is a passive process, meaning the loading efficiency is limited by the volume fraction of the liposomes. I-R1a concentrations in the size-sorted liposomes roughly matched that in the lipid rehydration buffer (10 μM).

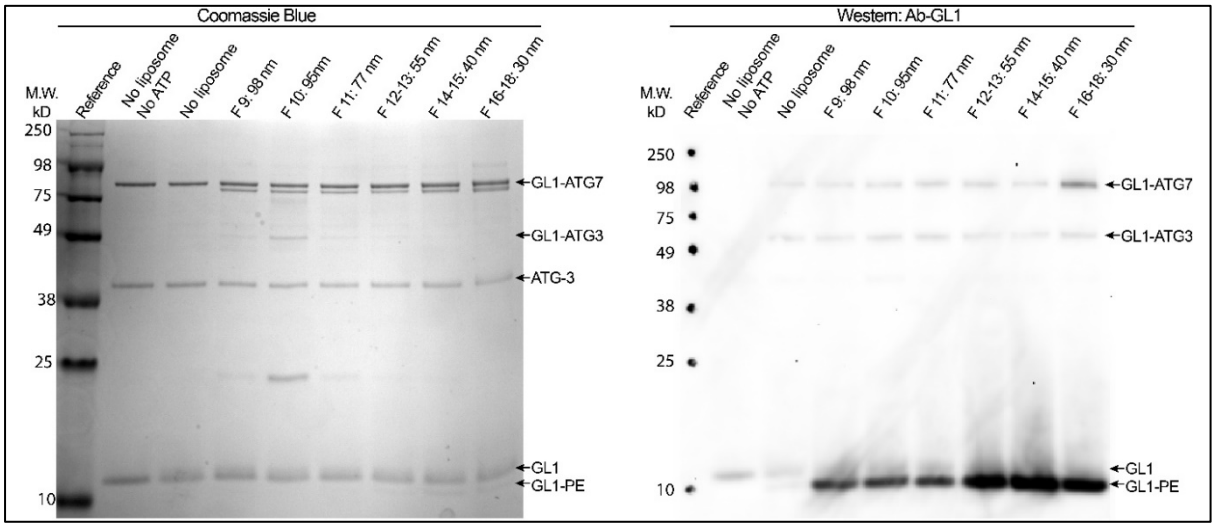

Supplementary Figure 19. Curvature dependency of ATG7/ATG3 catalyzed GL1 lipidation. Typical SDS-PAGE and western blot analyses of GL1 lipidation reactions are shown on the left and right panels, respectively. This experiment was repeated 5 times with similar results. Reaction conditions are summarized in Method **6**.

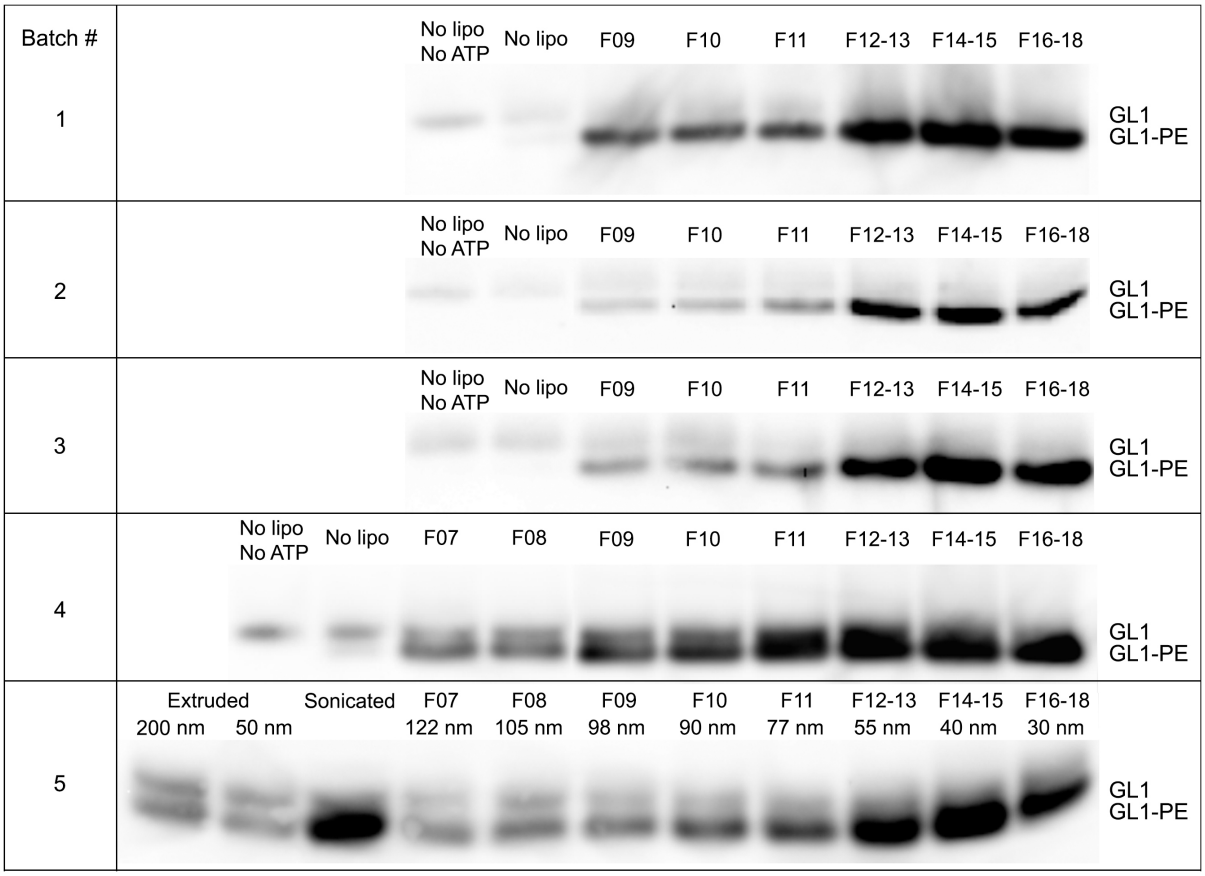

Supplementary Figure 20. ATG7/ATG3 catalyzed GL1 lipidation using sorted liposomes from five separate preparations (batch 1–5) analyzed by western blot.

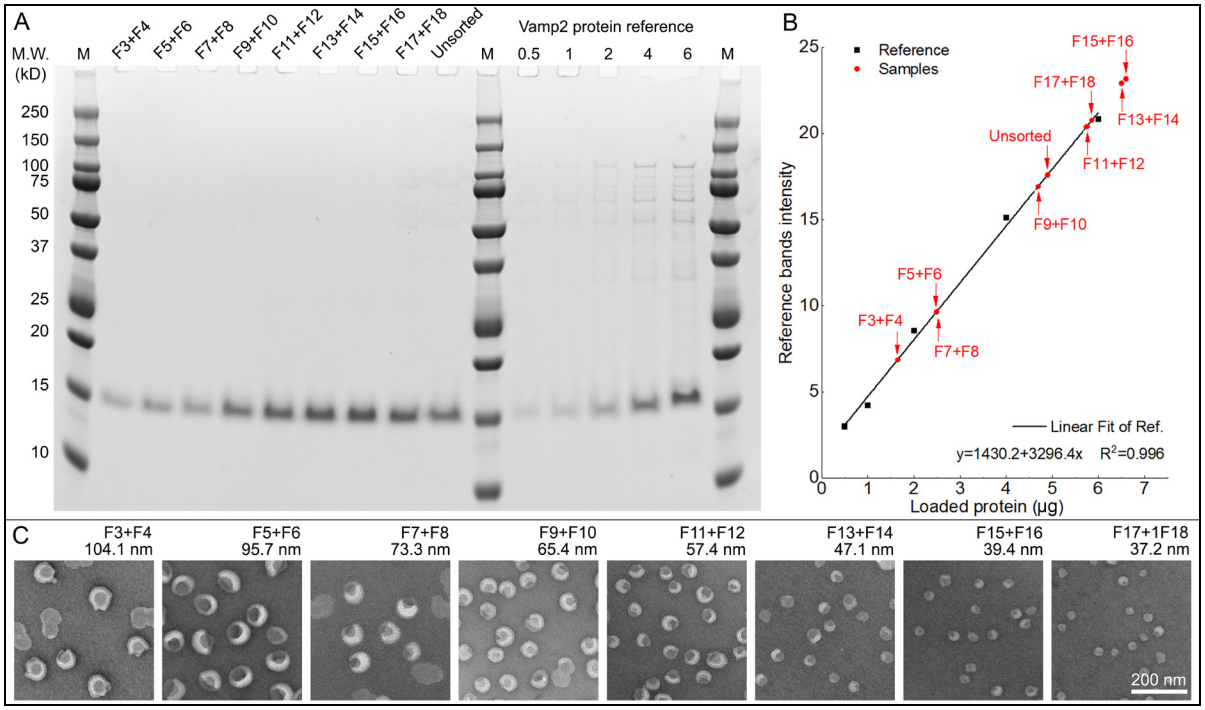

Supplementary Figure 21. Characterizations of proteoliposomes containing VAMP2. (A) and (B) Quantification of VAMP2 protein in reconstituted proteoliposomes before and after sorting. Liposomes reconstituted with VAMP2 are analyzed by SDS-PAGE alongside with protein concentration references (A). A linear regression of reference band intensity on the mass of proteins generates a calibration curve (B), which is used to calculate the amount of VAMP2 in the proteoliposomes before and after sorting. (C) Representative TEM images of VAMP2-containing liposomes after sorting. Fraction numbers and mean diameters on top of the corresponding TEM images. Scale bar: 200 nm. The experiments shown in (A) and (C) were repeated 6 and 5 times with similar results, respectively.

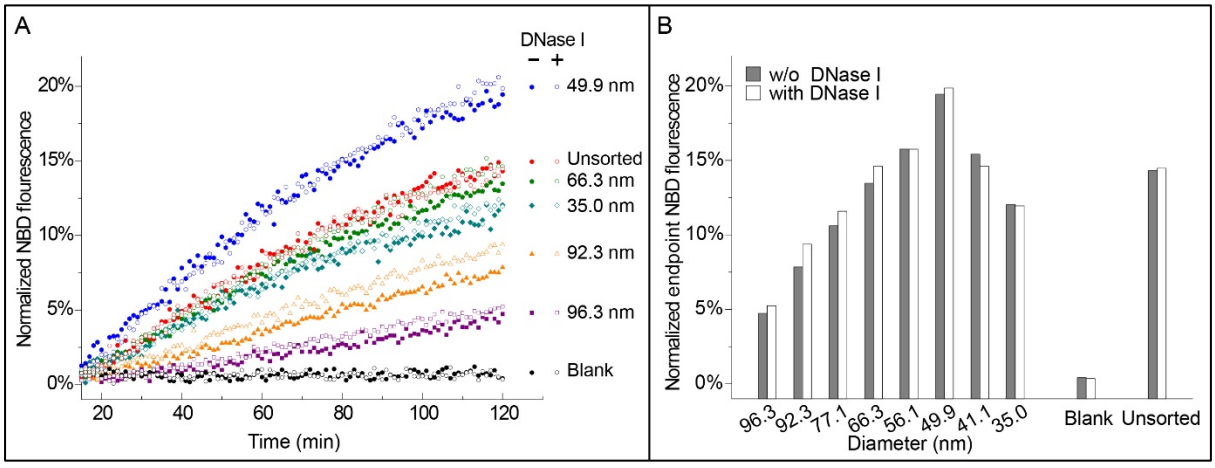

Supplementary Figure 22. Effect of membrane-bound DNA bricks on fusion assay. (A) NBD fluorescence traces showing the lipid mixing kinetics between unsorted t-SNARE liposomes and unsorted or sorted v-SNARE liposomes with or without DNase I digestion (1 U/10 μL, 37°C, 2 hours). (B) NBD fluorescence after 2 hours of fusion reactions (Method **7**, fluorescence traces shown in (A)).

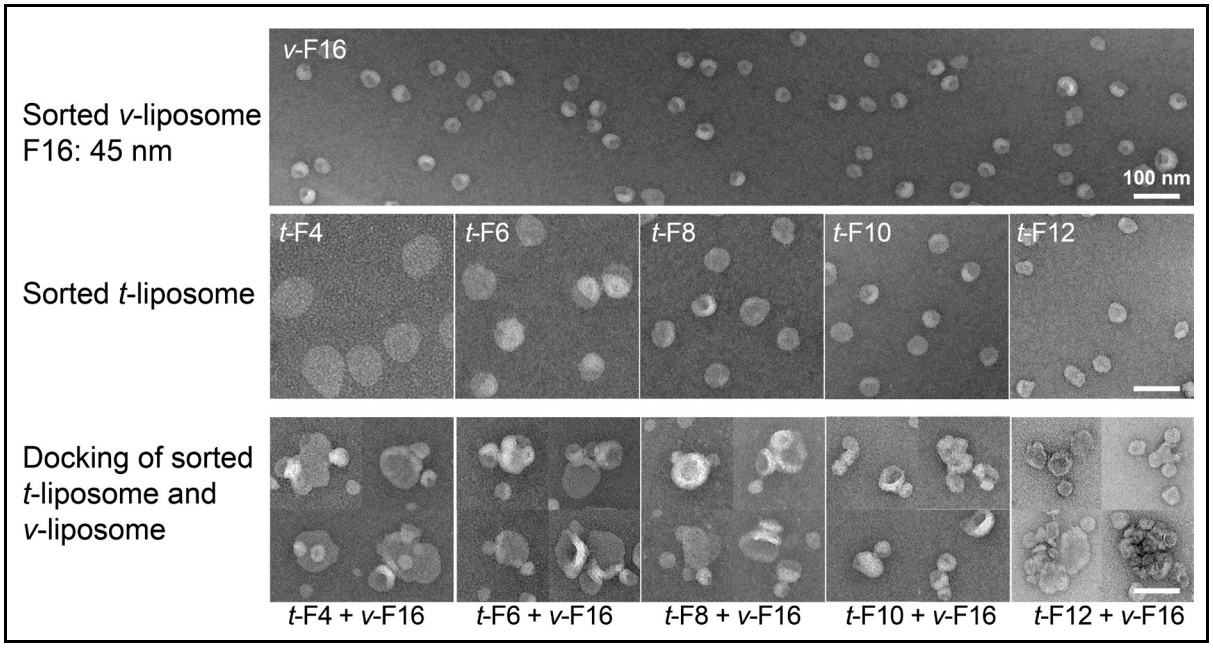

Supplementary Figure 23. Liposome docking in the pre-incubation period visualized by negative-stain TEM. Top row: a homogeneous population of v-SNARE liposomes after sorting (fraction 16, mean diameter: 45 nm). Middle row: t-SNARE liposomes sorted into five homogeneous populations (fractions 4, 6, 8, 10 and 12). Bottom row: incubating v-SNARE liposomes (45-nm mean diameter) and t-SNARE liposomes of various homogeneous sizes for 2 hours at 4°C (i.e., pre-incubation, see Method **7**) results in vesicle clusters, suggesting docking between the two proteoliposome species. Scale bars: 100 nm. This experiment was not repeated because of the time-consuming sample preparation.

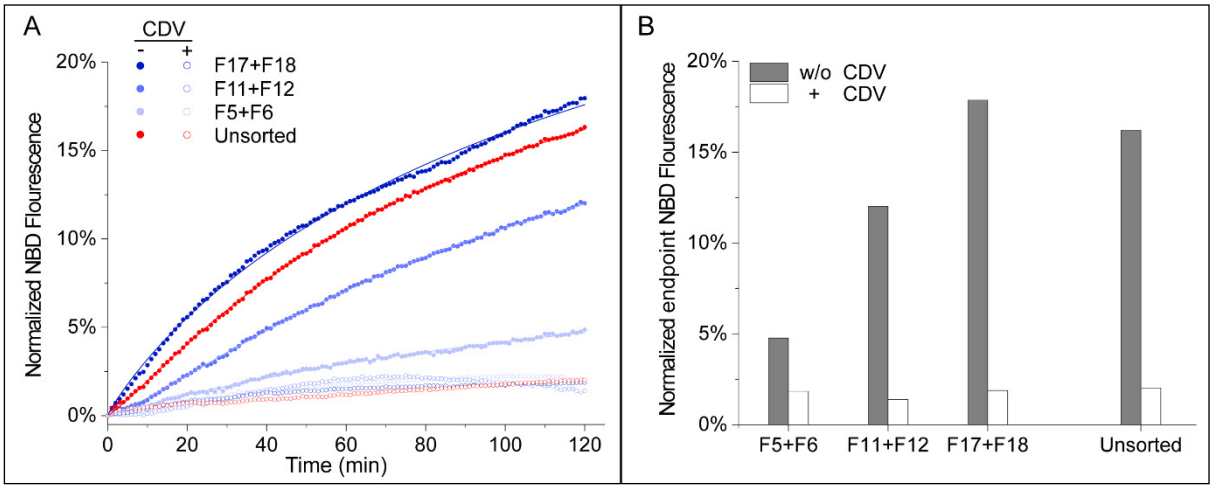

Supplementary Figure 24. Pre-inhibition of liposome fusion by soluble v-SNARE CDV (VAMP2 cytosolic domain, residues 1–94). See Method *7c*. (A) NBD fluorescence traces showing the lipid mixing kinetics between sorted and unsorted v-SNARE liposomes and unsorted t-SNARE liposomes with or without CDV treatment. The solid curves are a guide to the eye. (B) NBD fluorescence after 2 hours of fusion reactions.

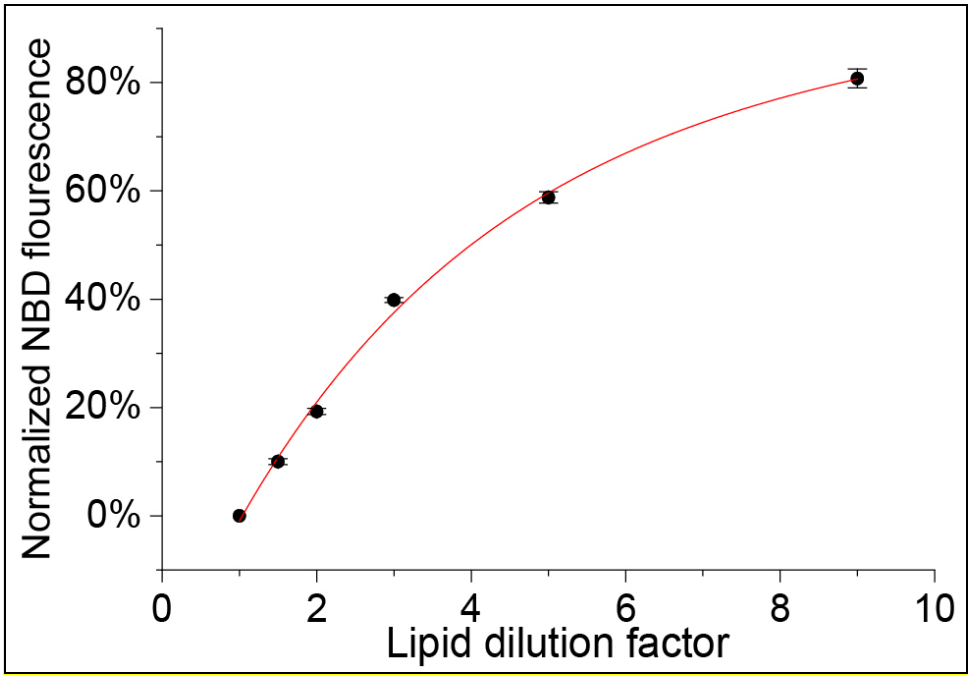

Supplementary Figure 25. A calibration curve that depicts the relationship between lipid dilution factor and normalized NBD fluorescence after fusion. Dots with error bars show the means and standard deviations of three trials. Red curve shows the result of bi-exponential fitting. See Method *7d* and **Supplementary Table 5**.

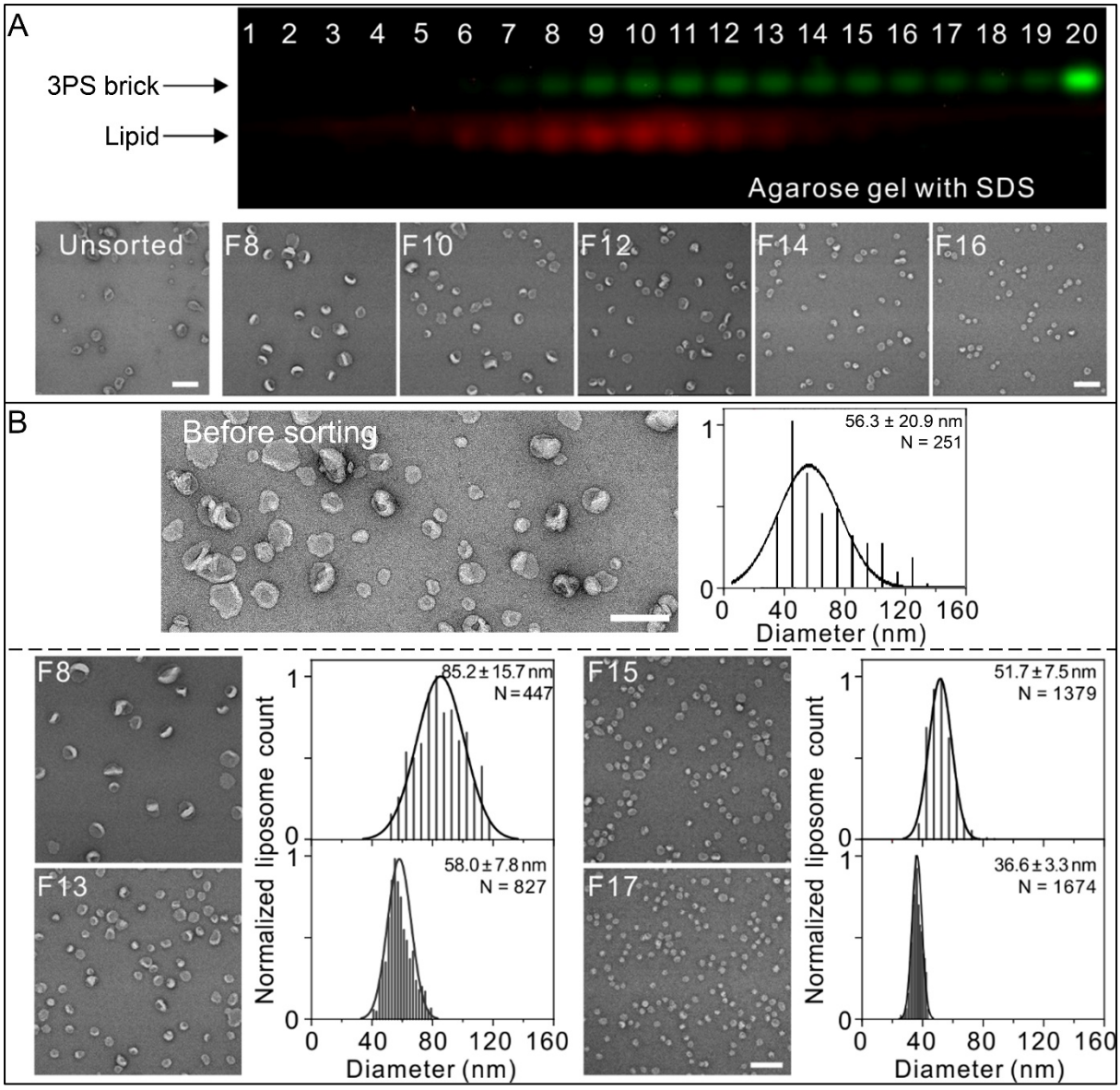

Supplementary Figure 26. Sorting experiment reproduced at Fudan University. (A) 3PS-brick-assisted sorting of liposomes (extruded through 50-nm filters, 0.4 μmol of total lipids) analyzed by SDS-agarose gel electrophoresis (top) and negative stain TEM (bottom). Fractions are numbered sequentially from F1 to F20 from top to bottom of the gradient. This experiment was repeated 3 times at Fudan with similar results. (B) The size distribution of unsorted (top) and sorted liposomes in selected fractions (F8, F13, F15 and F17, bottom) measured from negative-stain TEM images. Histograms are fitted to Gaussian curves. Fitted means and standard deviations (mean ± SD) of liposome diameters and sample sizes (N) are noted with the corresponding histograms. Scale bar: 200 nm.

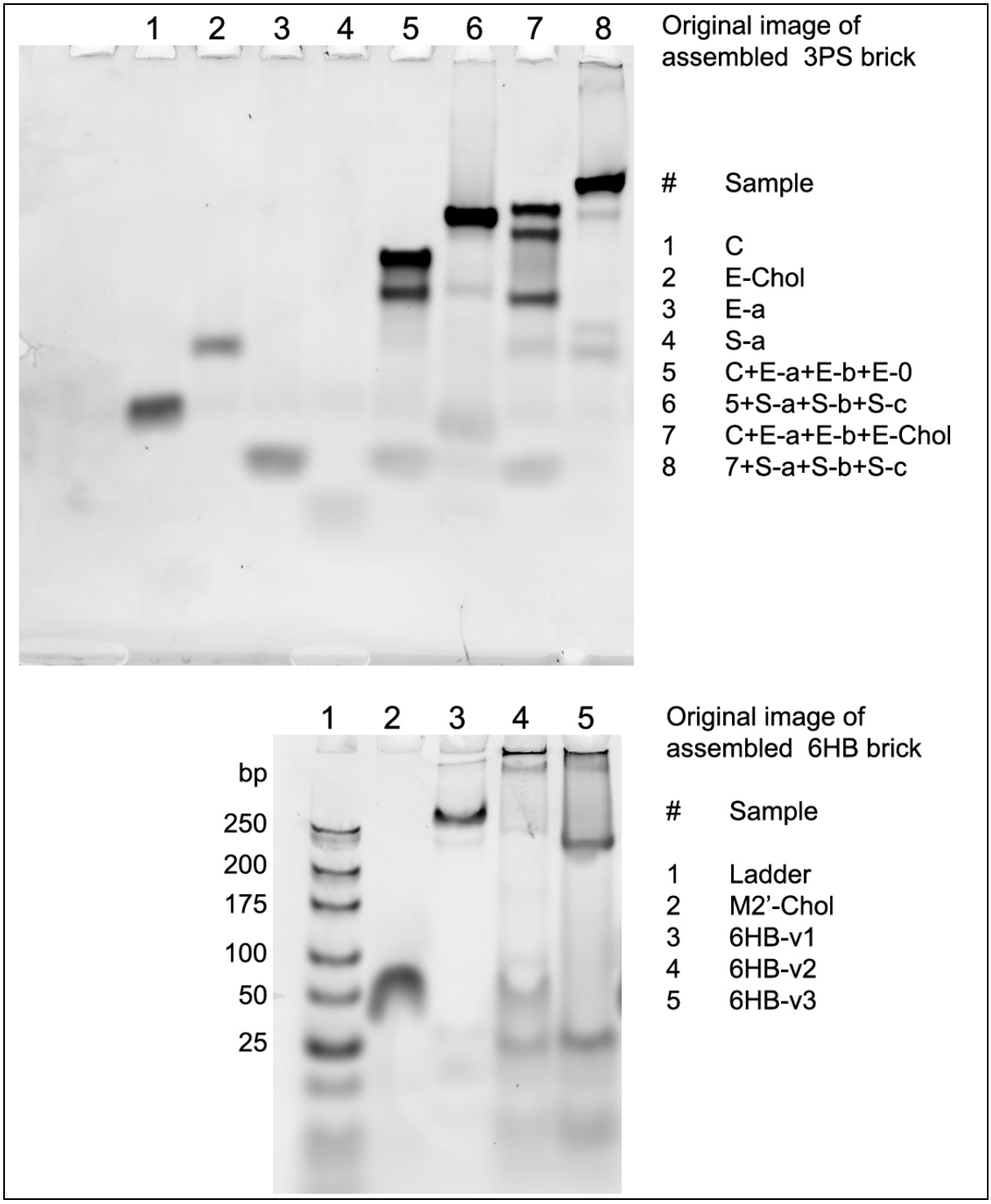

Supplementary Figure 27. The original, unprocessed gel images of the assembled DNA bricks as shown in **Supplementary Figure 1**. The oligonucleotide names noted on the side of the gel images can be found in **Supplementary Table 1**. Design of 6HB-v1 (**Supplementary Figure 1**) led to the highest assembly and liposome attachment efficiency and thus was used for the rest of the study. The 6HB-v2 was designed without the dT_3 overhangs at its cholesterol-carrying end and aggregated severely upon assembly. The 6HB-v3 was designed without the protruding 21-bp helix to carry the cholesterol anchor, which also led to noticeable DNA aggregation.

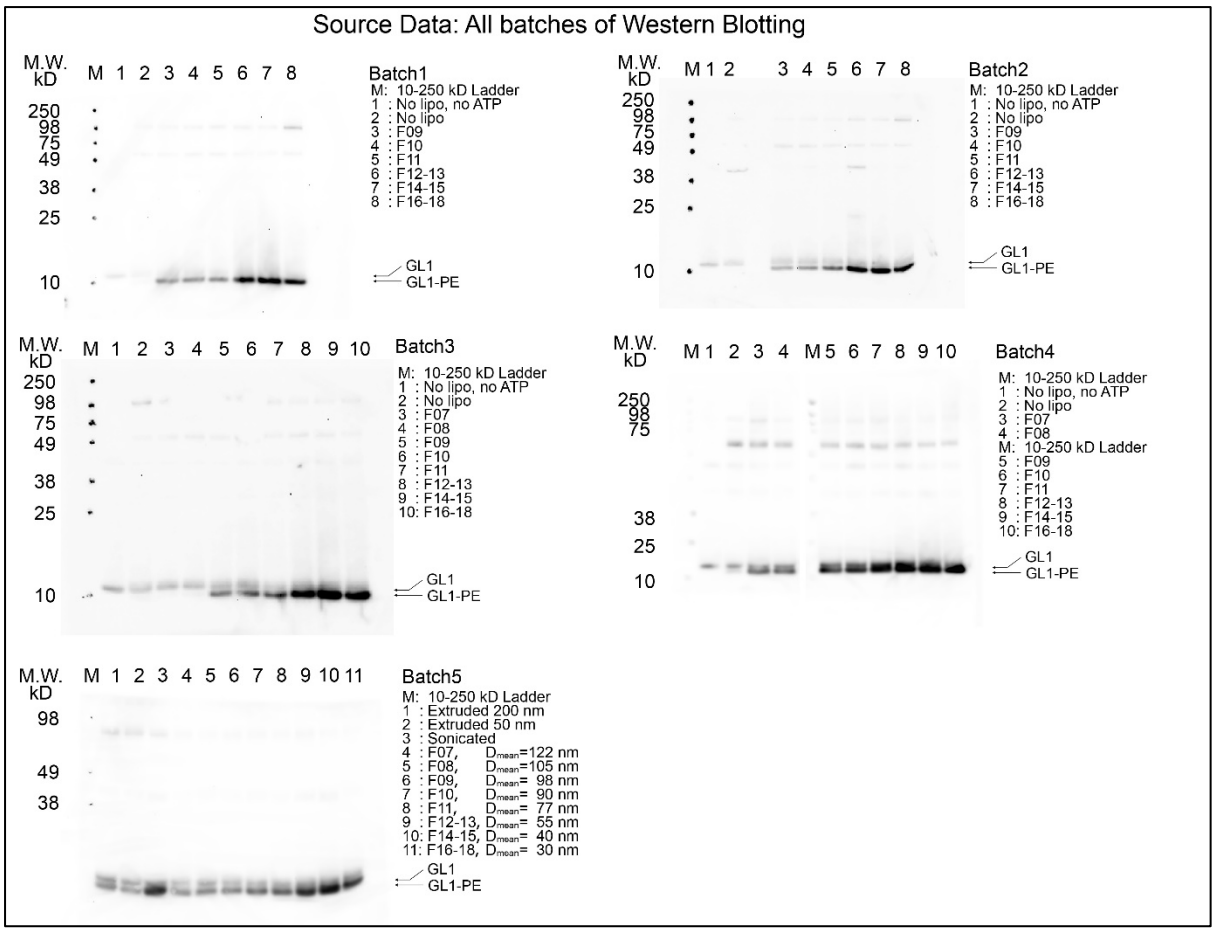

Supplementary Figure 28. The original, unprocessed western blots as summarized in **Supplementary Figure 20**.

Supplementary Notes

1. Material cost

A typical liposome sorting (20× scale in **Supplementary Table 1**) consumes 300 nmol lipid and 0.8 nmol DNA bricks. The material cost (in US$) is calculated as follows, based on the list prices provide by Integrated DNA Technologies, Inc. and Avanti polar lipids, Inc.

- Label-free oligonucleotides: $2.45 per base, 200 nmol final product per oligo
- Cholesterol-labeled oligonucleotide: $448 per strand, 25 nmol final product per oligo
- DOPC: $140 for 500 mg (635 μmol)
- DOPE: $420 for 500 mg (680 μmol)
- DOPS: $694 for 200 mg (124 μmol)
- 18:1 Liss Rhod PE: $474 for 10 mg (7.7 μmol)

3PS DNA brick (0.8 nmol):

[(Number of bases) × (synthesis cost per base per nmol) + (cholesterol-labeled oligo cost per nmol)] × (DNA bricks in nmol) / (assembly recovery yield) =
[(21×3×4+9-42) ×2.45/200+448/25]×0.8/90% = $18.3

6HB DNA brick (0.8 nmol)**:**

[(Number of bases) × (synthesis cost per base per nmol) + (cholesterol-labeled oligo cost per nmol)] × (DNA bricks in nmol) / (assembly recovery yield) =
[(42×6×2+21) ×2.45/200+448/25]×0.8/80% = $21.3

Lipids:

$\sum_{i=1}^{4}(\text{total lipid amount} \times \text{molar percentage(i)} \times \text{lipid price (i)})$ =
(300×0.592×140/635000+300×0.3×420/680000+300×0.1×694/124000+300×0.008×474/7700) = $0.41

Therefore, the total cost to sort liposomes containing 300 nmol lipid is $18.7 (using the 3PS brick) or $21.7 (using the 6HB brick). About 85% of the cost is for the synthesis of cholesterol-labeled oligonucleotides. Typically, at least 90% of liposomes can be recovered. The recovered amount of liposomes in a particular size range depends on such liposomes' abundance in the original mixture.

Compared with size-controlled liposomes generated by DNA-templated assembly method[1], which costs ~$30 for the preparation of liposomes containing 40 nmol of lipid, the sorting method generates liposomes with comparable size homogeneity at a fraction (<1/10) of the material cost.

Compared with conventional methods such as extrusion, the higher material and labor costs are justified by the superior size homogeneity (**Figure 1, Supplementary Figure 7** and **25**) and offset by the prolonged shelf-life of the DNA-coated liposomes (**Supplementary Figure 14**–**15**).

2. Fusion kinetics

Over the past few decades, all of the essential proteins and factors required for neuronal exocytosis have been identified. Notwithstanding these developments, we still lack empirical data concerning how positive membrane curvature, at the nm scale, facilitates fusion. Our results clearly show the acceleration of fusion over a specific range of increasing curvatures. However, we note that the smallest population of vesicles that we tested (<35 nm) did not appear to fuse with the fastest kinetics in the raw NBD dequenching traces. This is due to a number of confounding factors. First, the total number of v-SNAREs wane with decreasing

liposome size. Second, the lower density of v-SNAREs in the sub-35 nm vesicles is also likely to reduce fusion kinetics (**Figure 4c**). We therefore normalized the fusion rates (which were calculated by plotting rounds of fusion versus time) by both the surface area of v-SNARE liposomes and v-SNARE copy number. These corrections yielded a clear relationship between curvature and fusion rate (**Figure 4i**–**4j**). Interestingly, curvature was crucial factor only when liposomes were < 60–70 nm in diameter.

Reference

1 Yang, Y. *et al.* Self-assembly of size-controlled liposomes on DNA nanotemplates. *Nat Chem* **8**, 476-483 (2016).